Strong linkage between observed daily precipitation extremes and anthropogenic emissions across the contiguous United States

Nanditha J. S.[1], Gabriele Villarini[2], Hanbeen Kim[2], and Philippe Naveau[3]

[1]University of Iowa
[2]Princeton University
[3]IPSL-CNRS

April 19, 2024

Abstract

The results of probabilistic event attribution studies depend on the choice of the extreme value statistics used in the analysis, particularly with the arbitrariness in the selection of appropriate thresholds to define extremes. We bypass this issue by using the Extended Generalized Pareto Distribution (ExtGPD), which jointly models low precipitation with a generalized Pareto distribution and extremes with a different Pareto tail, to conduct daily precipitation attribution across the contiguous United States (CONUS). We apply the ExtGPD to 12 general circulation models from the Coupled Model Intercomparison Project Phase 6 and compare counterfactual scenarios with and without anthropogenic emissions. Observed precipitation by the Climate Prediction Centre is used for evaluating the GCMs. We find that greenhouse gases rather than natural variability can explain the observed magnitude of extreme daily precipitation, especially in the temperate regions. Our results highlight an unambiguous linkage of anthropogenic emissions to daily precipitation extremes across CONUS.

Hosted file

Manuscript1_final.docx available at https://authorea.com/users/543700/articles/740560-strong-linkage-between-observed-daily-precipitation-extremes-and-anthropogenic-emissions-across-the-contiguous-united-states

Hosted file

SI_GRL_final.docx available at https://authorea.com/users/543700/articles/740560-strong-linkage-between-observed-daily-precipitation-extremes-and-anthropogenic-emissions-across-the-contiguous-united-states

Strong linkage between observed daily precipitation extremes and anthropogenic emissions across the contiguous United States

Nanditha J. S.[1], Gabriele Villarini[2,3], Hanbeen Kim[2,3], Philippe Naveau[4]

[1]IIHR-Hydroscience and Engineering, University of Iowa, Iowa City, Iowa, USA

[2]Department of Civil and Environmental Engineering, Princeton University, Princeton, New Jersey, USA

[3]High Meadows Environmental Institute, Princeton University, Princeton, New Jersey, USA

[4]Laboratoire des Sciences du Climat et de l'Environnement, LSCE/IPSL, CNRS-CEA-UVSQ, Université Paris-Saclay, Gif-sur-Yvette, France

Abstract

The results of probabilistic event attribution studies depend on the choice of the extreme value statistics used in the analysis, particularly with the arbitrariness in the selection of appropriate thresholds to define extremes. We bypass this issue by using the Extended Generalized Pareto Distribution (ExtGPD), which jointly models low precipitation with a generalized Pareto distribution and extremes with a different Pareto tail, to conduct daily precipitation attribution across the contiguous United States (CONUS). We apply the ExtGPD to 12 general circulation models from the Coupled Model Intercomparison Project Phase 6 and compare counterfactual scenarios with and without anthropogenic emissions. Observed precipitation by the Climate Prediction Centre is used for evaluating the GCMs. We find that greenhouse gases rather than natural variability can explain the observed magnitude of extreme daily precipitation, especially in the temperate regions. Our results highlight an unambiguous linkage of anthropogenic emissions to daily precipitation extremes across CONUS.

Plain Language Summary

In this study, we investigate how human-induced emissions affect daily rainfall extremes across the United States. The attribution of an extreme event to human-induced emissions depends on the selected extreme event statistics, with setting a threshold to define what counts as an extreme event remaining a major challenge. To overcome this, we used the Extended Generalized Pareto

Distribution (ExtGPD) that jointly models both low and heavy rainfall events without defining a threshold, providing a more complete picture of the full distribution including extremes. We fitted the ExtGPD to 12 general circulation models and compared scenarios with and without human-induced emissions. Our findings suggest that human emissions are responsible for the observed intensity of daily rainfall extremes across the United States, especially in regions with temperate climates, and that these extremes would have been smaller without greenhouse gases.

Highlights

- We apply Extended Generalized Pareto Distribution for probabilistic event attribution as it bypasses issues with threshold specification.
- Anthropogenic emissions are responsible for the observed magnitude of extreme daily precipitation across the United States.
- The study underscores the urgent need for mitigation, revealing a clear link between anthropogenic activities and extreme precipitation.

1. Introduction

Climate attribution studies that examine the role of anthropogenic climate change in altering the probability of observed weather extremes have proliferated since Allen (2003), who proposed a simple probabilistic framework for detecting the role of anthropogenic forcing in the occurrence of an observed extreme. The availability of large ensemble climate model simulations and the Detection and Attribution Model Intercomparison Project (DAMIP) gave further impetus to climate attribution studies. The goal of these studies is to quantify the contribution of historic emissions and natural forcing in altering the risk of observed extremes and to project their changes (e.g., Gillett et al., 2016). This is generally accomplished using frequentist probabilistic methods (Oldenborgh (2021) and references therein). Most of these studies are event-specific attribution of observed extraordinary weather extremes in the recent years, while a few of them evaluate the role of anthropogenic emissions in altering the observed changes in extremes based on fingerprint techniques (e.g., Risser et al., 2022, Kirchmeier-Young & Zhang, 2020).

Previous studies have reported an observed intensification of precipitation extremes in the central and eastern parts of the contiguous United States (CONUS) and no detectable change is reported in the western United States (Easterling et al., 2017; Guo et al., 2019; Trenberth, 2018).

However, the existing event attribution studies have reported a low to medium confidence in human attribution to observed precipitation extremes across the CONUS (Seneviratne et al., 2021). For instance, event attribution studies found that the 3-day rainfall that caused the Louisiana floods of 2016 had become 40% more likely since 1900 (Van Der Wiel et al., 2017) and extreme precipitation associated with Hurricane Harvey in August 2017 in Houston was intensified due to global warming (e.g., Wang et al., 2018; Wehner & Sampson, 2021; Zhao et al., 2018). Similarly, external forcing reportedly caused the intensification and increased frequency of 1-day and 5-day annual maximum precipitation across North America based on optimal fingerprinting techniques (Kirchmeier-Young et al., 2020). On the other hand, an unequivocal role of human forcing was not detected in the 2013 Colorado heavy rainfall events (Hoerling et al., 2014; Pall et al., 2017). Most of the existing attribution studies are based on specific observed precipitation extremes spanning a few days in duration and impacting a specific region of interest. Moreover, the use of different approaches in the extreme event definition and statistical modelling makes a direct comparison of these studies difficult.

The definition of extremes is an important criterion in determining the apparent role of anthropogenic climate change (e.g. Philip et al., 2020). Kirchmeier-Young et al. (2019) suggested that longer spatial and temporal scales increase the signal-to-noise ratio of extreme weather events, making it easier to attribute longer- than shorter-scale events to human influences. The statistical approaches used for determining the changes in the frequency of extremes also influence the attribution statements (Naveau et al., 2020). The block maxima or peak-over-threshold (POT) approaches are usually employed to select the extreme events that are used for the subsequent statistical modelling. While a block maxima approach reduces the sample size of observed extremes to one per year, the POT method is constrained by the arbitrary choice of the threshold (e.g., Nerantzaki et al., 2023). The threshold selection in a POT method represents a tradeoff between ensuring an adequate sample size for statistical testing and adhering to the assumptions of extreme value distributions. The different approaches in event definition and arbitrary choice of thresholds make it difficult to interpret the existing studies. This necessitates the use of statistical approaches that are not dependent on threshold specification for climate attribution studies.

To address this issue, we employ the extended Generalized Pareto distribution (ExtGPD; Naveau et al., 2016), which jointly models low precipitation with a generalized Pareto distribution and heavy rainfall with a different Pareto tail, for building the statistical framework for climate attribution. The ExtGPD helps in modelling the entire range of data without the need for specifying a threshold, thereby increasing the sample size needed for fitting the statistical model. Here, we use the ExtGPD for providing a comprehensive statement on the role of anthropogenic forcing on altering the risk of daily precipitation extremes by sampling the entire precipitation time series across CONUS. We use counterfactual simulations from 12 general circulation models (GCMs) that participated in the DAMIP of the 6th Coupled Model Intercomparison Project (CMIP6) for generating the attribution statements. We organize the study into three sections: (1) evaluation of the performance of the GCMs in capturing daily precipitation extremes; (2) attribution of human contribution to daily precipitation extremes by comparing historical simulations with counterfactual scenarios; and (3) estimation of the sensitivity of anthropogenic forcing to the magnitude of extremes and climatic regions.

2. Data and Methods

2.1 Data

We used daily precipitation by the Climate Prediction Centre (CPC) available at 0.25° resolution over CONUS. For the evaluation and attribution study, we used 12 CMIP6 GCMs (Table S1) simulations from hist-nat, hist-GHG and historical scenarios. The hist-nat simulations are based on natural forcing (solar irradiation and volcanic aerosols) and exclude anthropogenic forcing (anthropogenic aerosols and emissions). The hist-GHG simulations are forced by well-mixed greenhouse gas emissions and exclude both natural and anthropogenic aerosols. The historical scenarios of GCMs are based on anthropogenic (GHG and aerosols) and natural forcing (volcanic and solar). The historical simulations of the GCMs are forced from 1850-2014 (Gillett et al., 2016). We used 34-year simulations from 1981-2014 to focus on the most recent decades and to mitigate potential issues related to the presence of non-stationarities. We regridded the CPC daily precipitation and climate model simulations to 1-degree resolution using bilinear interpolation to ensure consistency among the datasets. We excluded daily gridded precipitation below 0.1 mm of both CPC and CMIP6 datasets for the analysis to remove drizzle bias in the GCMs (e.g., Dai et al., 2006; DeMott et al., 2007).

2.2. Methods

2.2.1. Extreme value modelling

The generalized Pareto distribution (GPD) family is widely used for modelling extreme precipitation exceeding a particular threshold as it is appropriate for modelling heavy tail distributions (e.g., Coles, 2001) (equation 1); however, the threshold estimation is challenging. A large threshold could reduce the sample size and leads to higher uncertainty in the parameter estimations, while a smaller threshold does not satisfy the approximations of the GPD leading to model errors (e.g., Rivoire et al., 2021). Naveau et al. (2016) proposed a transition function to the GPD that provides a smooth connection between the upper tail and the main body of the function. This approach, called the extended GPD (ExtGPD), avoids the need for threshold specification and helps in sampling the entire timeseries for modelling extremes. This approach has been applied and tested in various contexts (e.g. Haruna et al., 2023; Gamet & Jalbert, 2022; Rivoire et al., 2021; Legrand et al., 2023).

The probability distribution of the GPD when the shape ξ (upper tail parameter) is larger than zero (i.e., heavy tail behavior) is:

$$H\left({}^{x}/_{\sigma}\right) = 1 - \left(1 + \frac{\xi x}{\sigma}\right)^{-1/\xi} \text{ for } \xi > 0 \qquad (1)$$

where, σ is the scale parameter of the GPD distribution and x is the random variable.

The ExtGPD is a transformation of the GPD, such that:

$$G(v) = v^{k} \text{ ; } where, v = H\left({}^{x}/_{\sigma}\right) \qquad (2)$$

and $k > 0$, is the lower tail parameter.

Naveau et al. (2016) proposed four different statistical formulations for the extended GPD model. We use the ExtGPD with three parameters (i.e., scale, lower tail parameter and the shape or upper tail parameter) owing to its simplicity and convergence of the statistical framework (equation 2). We estimate the parameters using the probability weighted moments method as it converges better than the maximum likelihood estimation (Naveau et al., 2016). We use the following initial values for the parameters: shape ξ = 0.2; scale, σ = 1; lower tail parameter, k = 0.5. We fit the ExtGPD to CPC and GCM daily precipitation values above 0.1 mm for each 1-

degree grid and estimate daily precipitation extremes of various return periods. We evaluate the performance of the GCMs in simulating observed precipitation based on the ability of the historical GCM simulations to capture CPC precipitation extremes: for each grid, we select only those models whose *n*-year return level of precipitation in historical simulations falls within the 95% confidence interval of the *n*-year return level of the CPC observations. Thus, we identify a subset of good-performing GCMs for each grid, which we use in the subsequent event attribution.

2.2.2. Climate attribution of extreme precipitation.

We use the 34-year counterfactual scenarios of hist-nat and hist-GHG (1981-2014) from the subset of GCMs to make a probabilistic attribution statement. We estimated the ratio of change in return level of extreme precipitation of the counterfactual scenarios to that of the historical simulations to quantify the impact of anthropogenic emissions (equation 3).

$$Attribution\ Ratio = \frac{P_{Counterfactual} - P_{historical}}{P_{historical}}, \tag{3}$$

where *counterfactual* stands for both hist–nat and hist–GHG.

A ratio greater (smaller) than zero implies that the counterfactual scenario increases (decreases) the *n*-year return level precipitation compared to the historical forcing. Further, we evaluate the sensitivity of the attribution ratio to different return periods and climate zones. The CONUS mainly falls within three climatic zones: arid, temperate and cold as per Köppen-Geiger climate classification (Beck et al., 2018). We separately assess the attribution ratio for each of the three climate zones. The analysis for the ExtGPD is performed in R using the mev and gmm libraries (Belzile, 2015; Chaussé, 2010).

3. Results

3.1. Evaluation of CMIP6 GCMs

We validated the performance of the GCMs by comparing their ability to capture the observed extremes. The spatial pattern of extremes is well captured by CESM2, CanESM5, E3SM-2-0, FGOALs-g3 and MRI-ESM2-0 (Figure 1b). The largest values in precipitation extremes based on CPC (Figure 1a) tend to be concentrated along the Gulf Coast and to decrease as we move inland northward, and on the Sierra Navada in the west; most GCMs can capture this gradient, even though some of them fail to do so. For instance, ACCESS-CM2, ACCESS-ESM1-5, BCC-CSM2-MR, GFDL-ESM4 and MIROC6 overestimate extremes in the central part of the study region. We observed the GCMs to perform well in simulating the extreme rainfall patterns in the U.S. Northeast, West Coast, the Great Plains of the North and South, and southeastern regions, which receive relatively high extreme precipitation (Figure 1). We also examined the performance of GCMs in capturing higher return level precipitation (Figures S1-S3) and found similar spatial patterns to those in the 100-year return period. Overall, most GCMs capture the spatial pattern of extreme precipitation across CONUS, even though a few of them overestimate extremes, limiting their use in subsequent modelling.

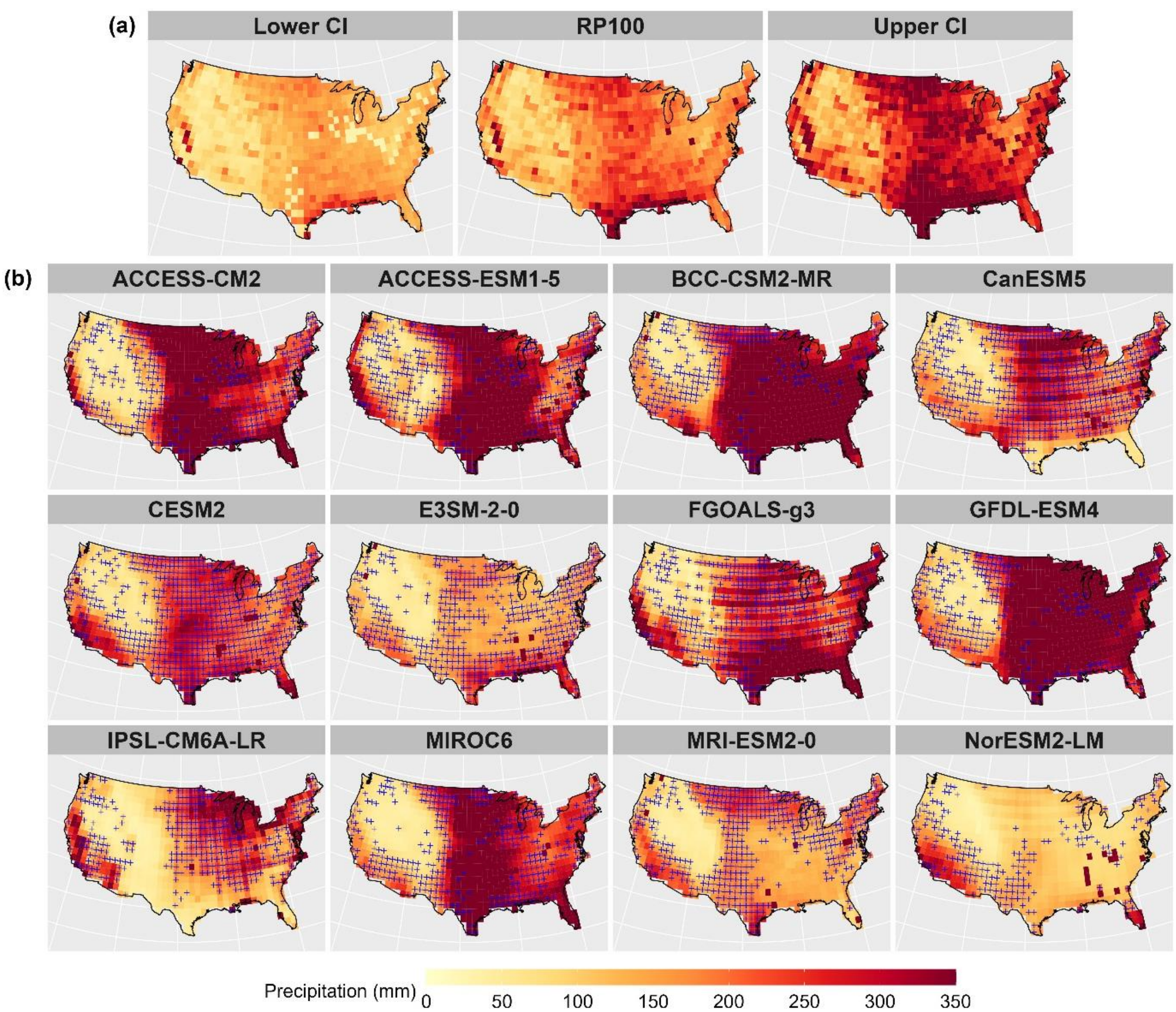

Figure 1. Evaluation of GCMs. Panels (a) show the 100-year daily precipitation (mm) and their upper and lower confidence interval (95% CI) based on CPC observations from 1981-2014.

Panels (b) show the 100-year daily precipitation extremes for the 12 GCMs from 1981-2014. The blue crosses highlight the grids that fall within the 95% CI of the CPC observations.

To mitigate issues with the biases in the estimates of extremes in certain GCMs, for the attribution we considered only those models whose *n*-year precipitation falls within the 95% confidence interval (CI) of the observations for each grid (Figure 1b). This approach helps in removing the GCMs that significantly underestimate or overestimate the observed precipitation pattern, helping to reduce the uncertainty in climate attribution statements. More than five GCMs satisfy the above condition in most grids across CONUS, with the highest number of GCMs available in the western and central United States, as well as the northeastern regions (Figure S4). At least three GCMs with satisfactory performance are available in more than 87% grids (730 grids of the total 831 grids) across CONUS, thereby ensuring the robustness of the estimates. In short, over five GCM simulations of *n*-year return level precipitation are consistent with the corresponding CPC simulation of precipitation extremes across most of the CONUS and we use them for climate attribution (Figure S4). Moreover, the whole time series of precipitation (>0.1 mm) are sampled by fitting the ExtGPD distribution. Therefore, the comparison of extremes in CMIP6 GCMs and CPC observations provides more confidence in the GCM precipitation simulations.

3.2. Climate attribution

We estimate the attribution ratio by taking the ratio of the change in return level in the counterfactual scenario (hist-nat and hist-GHG) to that of the historical simulations (equation 3). We estimate the multi-model mean attribution ratio of the subset of GCMs that performed well compared to CPC for each grid based on 100-year precipitation (Figure 2 and Figures S6-S7). Most regions across the country exhibit an attribution ratio below 0 in the hist-nat scenario and above 0 in the hist-GHG scenario (Figure 2). The results show a counterfactual scenario of natural-only forcing would have made the 100-year daily precipitation event smaller than the observations (Figure 2). Likewise, a well-mixed greenhouse gas emission scenario that excludes both anthropogenic and natural aerosols would have enhanced the 100-year daily precipitation extremes during the observational period (Figure 2). We observed consistent patterns in the attribution ratio at higher return levels of daily precipitation (Figure S8). Overall, we identify the significant role of anthropogenic emissions in exacerbating the daily precipitation extremes across the CONUS.

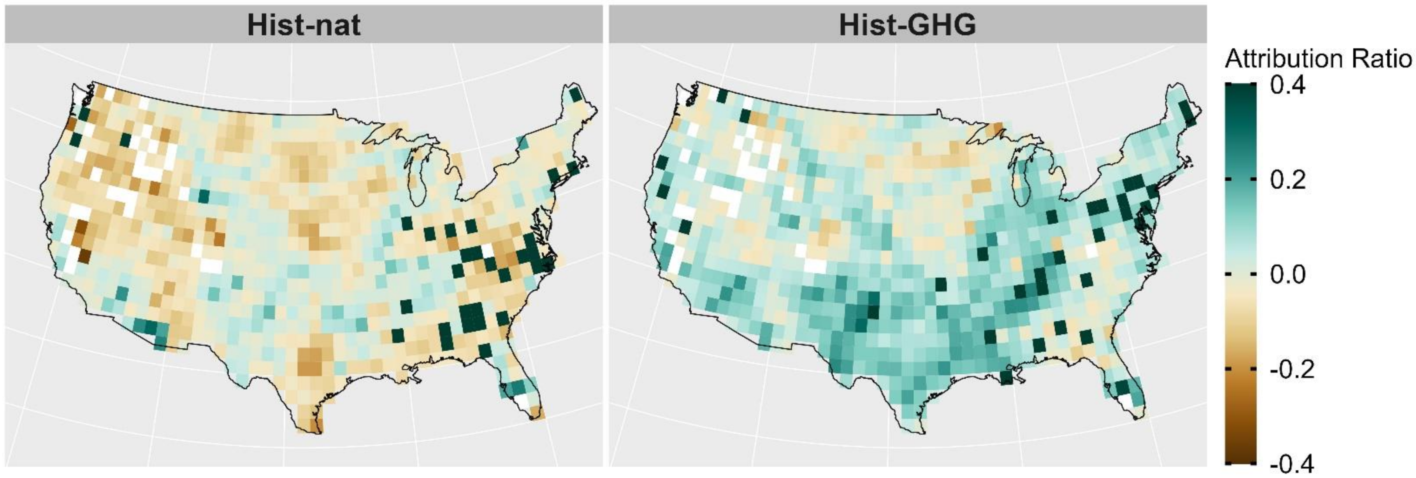

Figure 2. Multi-model mean attribution ratio of hist-nat and hist-GHG simulations estimated using the subset of GCMs that performed well with respect to CPC for the 100-year daily precipitation. For each grid, the mean is estimated based on the GCMs that capture the observed extremes (Figure S4). The white color corresponds to grids for which all GCMs failed to capture the observed extremes within the 95% confidence interval.

Five or more GCMs that captures the historical extremes are considered for computing the multi-model mean attribution ratio in most grids (Figure S4). We compared the sign of the attribution ratio of the subset of GCMs in each grid to assess the robustness of the estimates of different GCMs. The majority of the GCMs shows a negative sign of change in the hist-nat scenario and a positive sign of change in the hist-GHG scenario (Figures S5-S7). We found that a high percentage of GCMs agree in the sign of change at regions with high strength in attribution (Figure 2 and Figure S5). The Northwest, U.S. East Coast, Midwest and southern regions show a high negative attribution ratio and have a high percentage of GCMs agreeing on the sign of change (negative attribution ratio) in the hist-nat scenario (Figure 2 and Figure S5). Similarly, the Southern Plains, the east-central United States, U.S. Northeast and West Coast show high positive attribution ratio and have a higher percentage of GCMs agreeing on the positive sign of change (Figures 2 and Figure S5). Thus, the grids with higher magnitude of the multi-model mean attribution ratio have more GCMs that agree on the sign of change, making the result robust across the GCMs. The higher magnitude of extreme precipitation in a GHG-only scenario (hist-GHG) compared to the historical simulations highlights the modulating effect of natural and anthropogenic aerosols in reducing precipitation intensities. Aerosols, particularly sulphate aerosols, have a net negative impact on radiative forcing due to their high reflectance and indirect effect on cloud formation, leading to a reduction in precipitation (e.g., Allan et al., 2020; Risser et al., 2022). The positive attribution ratio in the hist-GHG also coincides with regions with high sulphate aerosols emissions across CONUS, including the northeastern, the east-central and southwestern United States and the U.S. West Coast (Risser et al., 2022). The increased risk of extreme daily precipitation in the hist-GHG scenario can be attributed to not accounting for the role of aerosols. A lower daily precipitation magnitude in the natural-forcing scenario emphasizes the role of GHG emissions in exacerbating the precipitation extremes. We have not directly compared the precipitation magnitudes in the two counterfactual scenarios of well-mixed GHG and natural only forcing. However, it is evident that GHG forcing alone would have enhanced the magnitude of observed extremes compared to natural forcing (Figure 2 and Figures S6-S7).

We observed distinct regional patterns in the attribution ratio. The Southern Plains, eastern-central and north-eastern United States, which receive intense precipitation, exhibit a higher sensitivity of precipitation extremes to anthropogenic forcing (right panel in Figures 1a and 2). On the contrary, the western United States, including the U.S. Northwest and the Northern Plains, show a higher reduction in extremes under natural-only forcing (left panel in Figure 2). This is consistent with the spatial pattern of observed extreme precipitation across CONUS (Figure 1a). An intensification of heavy precipitation is observed since 1979 in the central and eastern United States, attributed to the increased frequency of mesoscale convective systems that cause heavy precipitation during the warm season (Easterling et al., 2017). Similarly, a linear increase in precipitation extremes is reported in the Midwest, U.S. East Coast and the Great Plains excluding the northwest regions (Dong et al., 2021), with a low confidence in the increase of extreme precipitation in the western regions (Seneviratne et al., 2021). Overall, we found the Southern Plains and the northeast regions, which receive intense daily precipitation and an observed increase in extremes, are highly sensitive to anthropogenic GHG emissions, more so than some of the drier northwestern regions.

3.3. Role of climate patterns and return period on the attribution ratio

We observed regional variability in the attribution ratio under the two counterfactual scenarios. To understand the role of climatic regions on the attribution ratio, we estimated the multi-model mean attribution ratio for the three major Köppen-Geiger climate classes over CONUS, namely arid, cold and temperate regions (Beck et al., 2018). The temperate regions exhibit the highest increase in extreme precipitation under hist-GHG simulations, followed by the arid regions, with the areas belonging to the cold region showing the lowest signal (Figure 3). The vast number of event attribution studies conducted in the southern and central United States highlights the role of anthropogenic emissions in increasing the probability of observed precipitation extremes in the temperate eastern United States (Van Der Wiel et al., 2017; Wang et al., 2018; Zhao et al., 2018), consistent with our findings. In the hist-nat scenario, the temperate and arid regions show a relatively low decrease in precipitation extremes compared to the cold regions, which show the highest decrease (Figure 3). Moreover, the cold regions have the smallest interquartile spread in the attribution ratio in the hist-nat scenario. However, the difference among the climatic regions is much less in hist-nat compared to hist-GHG scenario. As observed earlier, the arid and cold regions, which received low precipitation extremes during the study period, have a low attribution ratio compared to the temperate regions in the hist-GHG scenario, which receive intense daily precipitation. This implies that GHG emissions exacerbate precipitation extremes in wetter regions compared to drier ones.

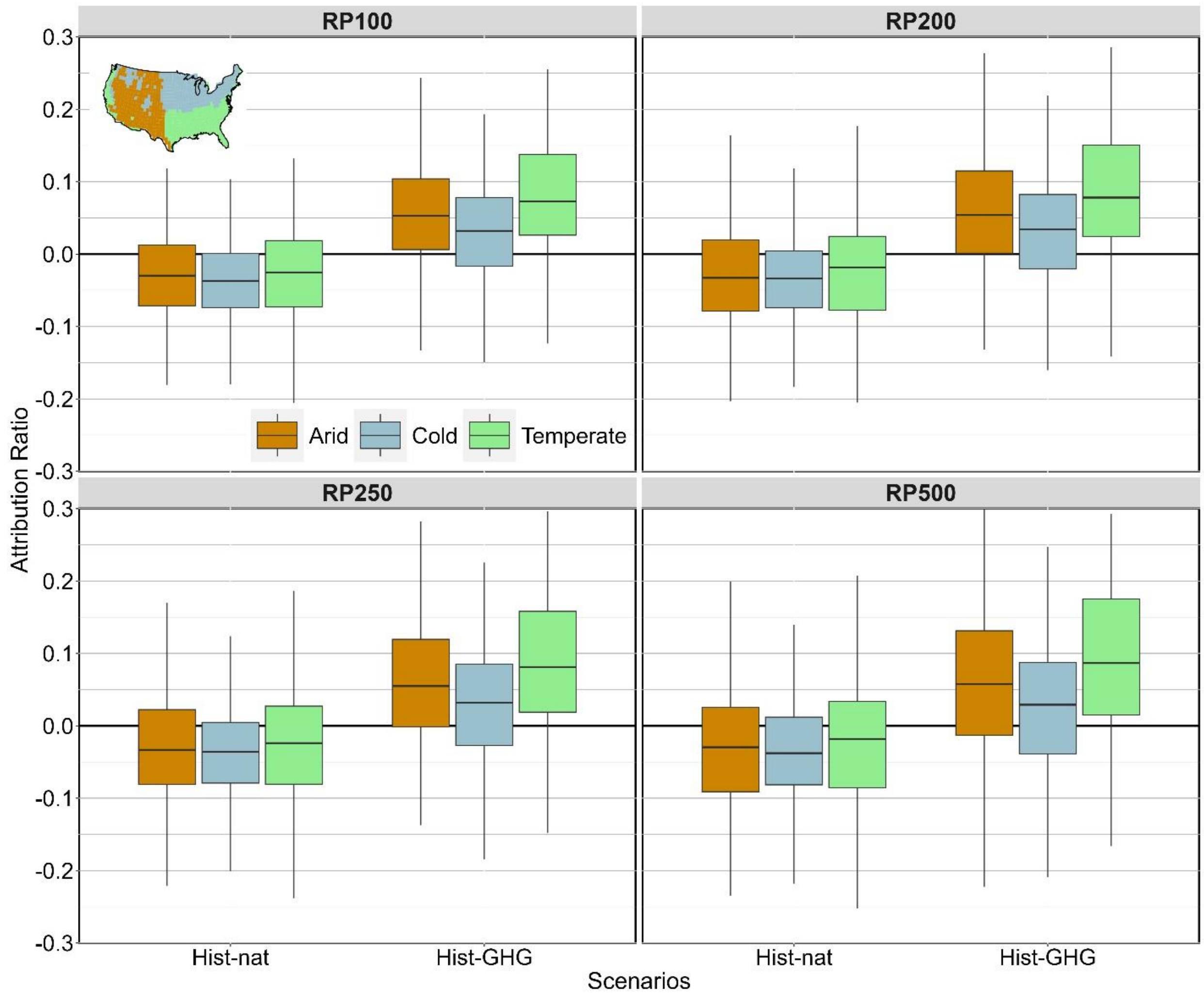

Figure 3. Attribution ratio for the three main Köppen-Geiger climate classes across CONUS. The spatial extent of the three main climate classes (arid, cold, and temperate) is shown in the inset figure. The box plots depict the attribution ratio for the three climate classes in a hist-nat and hist-GHG scenario for 100, 200, 250 and 500-year daily precipitation. In the boxplots, the dark horizontal line represents the median, the box represents the interquartile range, and the whiskers correspond to the 5th and 95th percentile values.

We also compared the sensitivity of the attribution ratio to the magnitude of the extremes. We observed a slight increase in the risk of extreme precipitation of higher return periods (RP=200, 250, 500) due to anthropogenic emissions (Figure 3 and Figures S8-S9). There is a nominal increase (decrease) in the multi-model mean attribution ratio in the hist-GHG (hist-nat) scenario with an increase in precipitation return period (Figure 3 and Figure S8). However, there is a substantial increase in the interquartile range as the return period increases (Figure 3 and Figure

S9). The temperate climatic regions exhibit a relatively higher increase in the attribution ratio in the hist-GHG scenario compared to the hist-nat (Figure 3). Overall, we find that the likelihood of higher magnitude precipitation extremes would have increased in a counterfactual scenario of anthropogenic emissions compared to the historical scenario. Previous studies outline that the probability of rare extremes increases at a higher rate in a warming world (Myhre et al., 2019), in agreement with our results, even though at a more muted level.

4. Discussion and Conclusions

We used the ExtGPD to assess the performance of 12 DAMIP GCMs in capturing the daily precipitation extremes. Unlike the GPD, the ExtGPD samples the entire time series and removes the arbitrariness in threshold selection in modelling extremes. Hence, the comparison of CPC observations and GCMs using the ExtGPD provides a robust estimation of the climate model performance, and we found that most GCMs capture the spatial pattern of observed extremes. Our probabilistic attribution study shows an unambiguous connection of human emissions to daily precipitation extremes across CONUS. We report higher confidence in the attribution of daily precipitation extremes to well-mixed GHG emissions in the Northeast, Southern Plains, and U.S. West Coast, which receive high extreme precipitation, consistent with previous studies (e.g., Easterling et al., 2017, Dong et al., 2016). The arid regions in the west and the colder Midwest show a higher sensitivity to a counterfactual scenario of natural forcing, implying a reduction in extreme precipitation magnitude compared to the observed extremes. The spatial distribution of the attribution ratio identified in the study aligns with the observed pattern of precipitation extremes, suggesting a tendency for increased extreme magnitudes in regions experiencing higher levels of extremes.

One limitation of this study is the lower spatial resolution of the DAMIP GCMs (~120 km), which leads to an inherent disadvantage in the accurate simulation of the regional precipitation patterns. However, the attribution ratio defined in the study is based on the counterfactual scenarios of the same climate models forced with different external forcings. Therefore, assuming that the response of the GCMs to the anthropogenic and natural forcing would be the same across resolutions, then our attribution statements would not be impacted by their coarse resolution. This assumption should be verified in future studies using a suite of models with different resolutions. To strengthen our results and lend more credence to their robustness, we only considered a subset of GCMs that performed well in reproducing the observed statistical properties of rainfall extremes, and used the ExtGPD, which samples the entire time series with no need for thresholds.

Anthropogenic warming has already increased the global mean temperature by 1°C from the pre-industrial level and the current emission trajectory is expected to exceed 1.5°C by the middle of the 21st century (Masson-Delmotte et al., 2018). An increase in global mean temperature increases the water holding capacity of the atmosphere according to the Clausius Clapeyron relationship, which in turn increases the frequency of precipitation extremes (Allan & Soden, 2008; Fowler et al., 2021; Papalexiou & Montanari, 2019; Westra et al., 2014). Our results highlight the human influence on observed daily precipitation extremes across CONUS and emphasize the need for active reduction in human emissions to mitigate the intensification of precipitation extremes in future.

Acknowledgements: We acknowledge the availability of CPC Unified Gauge-Based Analysis of Daily Precipitation over CONUS data provided by the NOAA PSL, Boulder, Colorado, USA, from their website at https://psl.noaa.gov. We acknowledge the World Climate Research Programme, which, through its Working Group on Coupled Modelling, coordinated and promoted CMIP6. We thank the climate modeling groups for producing and making available their model output, the Earth System Grid Federation (ESGF) for archiving the data and providing access, and the multiple funding agencies who support CMIP6 and ESGF. This work was in part funded by Princeton University. Part of Philippe Naveau's work was supported by three French national programs (PEPR TRACCS ANR, 80 PRIME CNRS-INSU; ANR T-REX under reference ANR-20-CE40-0025-01) and the European H2020 XAIDA project (grant agreement no. 101003469).

Open Research: The CPC and CMIP6 multi-model precipitation data used in the study are freely downloadable from https://psl.noaa.gov/data/gridded/data.unified.daily.conus.html and https://esgf-data.dkrz.de/search/esgf-dkrz/, respectively. The CMIP6 models used in the study are listed in Table S1. The analysis in this study is performed in R, an open-source computational software. The codes used for the analysis and data visualization are made available at *http://www.hydroshare.org/resource/d372565acce441bebdd49a0cf0307ff3*.

Declaration of Competing Interest: The authors declare no competing personal relationships or financial interests that could have appeared to influence the work reported in this paper.

Author Contribution: Nanditha J. S.: Methodology, Software, Formal analysis, Investigation, Data curation, Writing – original draft, Writing – review & editing, Visualization. Gabriele Villarini: Conceptualization, Methodology, Investigation, Writing – review & editing, Supervision, Project administration, Funding acquisition. Hanbeen Kim: Software, Writing – review & editing, Visualization. Philippe Naveau: Investigation, Writing – review & editing

References

Abubakar Haruna, Juliette Blanchet, and Anne-Catherine Favre. Modeling intensity-duration-frequency curves for the whole range of non- zero precipitation: A comparison of models. Water Resources Research, 59(6):e2022WR033362, 2023.

Allan, R. P., & Soden, B. J. (2008). Atmospheric warming and the amplification of precipitation extremes. *Science*, *321*(5895), 1481–1484. https://doi.org/10.1126/science.1160787

Allan, R. P., Barlow, M., Byrne, M. P., Cherchi, A., Douville, H., Fowler, H. J., et al. (2020). Advances in understanding large-scale responses of the water cycle to climate change. *Annals of the New York Academy of Sciences*. https://doi.org/10.1111/nyas.14337

Allen, M. R., & Ingram, W. J. (2002). Constraints on future changes in climate and the hydrologic cycle. *Nature 2002 419:6903*, *419*(6903), 228–232. https://doi.org/10.1038/nature01092

Allen, M. (2003). Liability for climate change. *Nature, 421*(6926), 891-892.

Bao, J., Sherwood, S. C., Alexander, L. V., & Evans, J. P. (2017). Future increases in extreme precipitation exceed observed scaling rates. *Nature Climate Change*, *7*(2), 128–132. https://doi.org/10.1038/nclimate3201

Beck, H. E., Zimmermann, N. E., McVicar, T. R., Vergopolan, N., Berg, A., & Wood, E. F. (2018). Present and future Köppen-Geiger climate classification maps at 1-km resolution. Scientific data, 5(1), 1-12.

Belzile, Leo, Jennifer L. Wadsworth, Paul J. Northrop, Scott D. Grimshaw, Jin Zhang, Michael A. Stephens, Art B. Owen, Raphael Huser, and Maintainer Leo Belzile. "Package ‘mev’." (2015).

Chaussé, P. (2010), Computing generalized method of moments and generalized empirical likelihood with R, J. Stat. Software, 34-11, 1–35.

Dai, A. (2006). Precipitation characteristics in eighteen coupled climate models. *Journal of Climate*, *19,* 4605–4630. https://doi.org/10.1175/JCLI3884.1

DeMott, C. A., Randall, D. A., & Khairoutdinov, M. (2007). Convective precipitation variability as a tool for general circulation model analysis. *Journal of Climate, 20*, 91–112. https://doi.org/10.1175/JCLI3991.1

Dong, S., Sun, Y., Li, C., Zhang, X., Min, S. K., & Kim, Y. H. (2021). Attribution of extreme precipitation with updated observations and CMIP6 simulations. *Journal of Climate*, *34*(3), 871–881. https://doi.org/10.1175/JCLI-D-19-1017.1

Easterling, D. R., Arnold, J. R., Knutson, T., Kunkel, K. E., LeGrande, A. N., Leung, L. R., et al. (2017). *Ch. 7: Precipitation Change in the United States. Climate Science Special Report: Fourth National Climate Assessment, Volume I*. Washington, DC. https://doi.org/10.7930/J0H993CC

Eden, J. M., Wolter, K., Otto, F. E. L., & Jan Van Oldenborgh, G. (2016). Multi-method attribution analysis of extreme precipitation in Boulder, Colorado. *Environmental Research Letters*, *11*(12). https://doi.org/10.1088/1748-9326/11/12/124009

Fowler, H. J., Lenderink, G., Prein, A. F., Westra, S., Allan, R. P., Ban, N., et al. (2021). Anthropogenic intensification of short-duration rainfall extremes. *Nature Reviews Earth & Environment 2021 2:2*, *2*(2), 107–122. https://doi.org/10.1038/s43017-020-00128-6

Gillett, N.P., Shiogama, H., Funke, B., Hegerl, G., Knutti, R., Matthes, K., Santer, B.D., Stone, D. and Tebaldi, C., 2016. The detection and attribution model intercomparison project (DAMIP v1. 0) contribution to CMIP6. *Geoscientific Model Development*, *9*(10), pp.3685-3697.

Guo, R., Deser, C., Terray, L., & Lehner, F. (2019). Human Influence on Winter Precipitation Trends (1921–2015) over North America and Eurasia Revealed by Dynamical Adjustment. *Geophysical Research Letters*, *46*(6), 3426–3434. https://doi.org/10.1029/2018GL081316

Juliette Legrand, Pierre Ailliot, Philippe Naveau, and Nicolas Raillard. Joint stochastic simulation of extreme coastal and offshore significant wave heights. Ann. Appl. Statist., 17(4):3363–3383, 2023.

Kirchmeier-Young, M. C., Wan, H., Zhang, X., & Seneviratne, S. I. (2019). Importance of Framing for Extreme Event Attribution: The Role of Spatial and Temporal Scales. *Earth's Future*, *7*(10), 1192–1204. https://doi.org/10.1029/2019EF001253

Kirchmeier-Young, Megan C., & Zhang, X. (2020). Human influence has intensified extreme precipitation in North America. *Proceedings of the National Academy of Sciences of the United States of America*, *117*(24), 13308–13313. https://doi.org/10.1073/PNAS.1921628117/SUPPL_FILE/PNAS.1921628117.SAPP.PDF

Marvel, K., & Bonfils, C. (2013). Identifying external influences on global precipitation. *Proceedings of the National Academy of Sciences of the United States of America*, *110*(48), 19301–19306. https://doi.org/10.1073/pnas.1314382110

Masson-Delmotte, V., P. Z., Pörtner, H.-O., Roberts, D., Skea, J., Shukla, P. R., et al. (2018). *IPCC, 2018: Summary for Policymakers. In: Global Warming of 1.5°C. An IPCC Special Report on the impacts of global warming of 1.5°C above pre-industrial levels and related global greenhouse gas emission pathways, in the context of strengthening the global*. *Global Warming of 1.5°C*. Cambridge, UK and New York, NY, USA,. https://doi.org/https://doi.org/10.1017/9781009157940.001

Myhre, G., Alterskjær, K., Stjern, C.W., Hodnebrog, Ø., Marelle, L., Samset, B.H., Sillmann, J., Schaller, N., Fischer, E., Schulz, M. and Stohl, A., 2019. Frequency of extreme precipitation increases extensively with event rareness under global warming. *Scientific reports*, *9*(1), p.16063.

Naveau, P., Huser, R., Ribereau, P., & Hannart, A. (2016). Modeling jointly low, moderate, and heavy rainfall intensities without a threshold selection. *Water Resources Research*, *52*(4), 2753–2769. https://doi.org/10.1002/2015WR018552

Naveau, P., Hannart, A., & Ribes, A. (2020). Statistical methods for extreme event attribution in climate science. *Annual Review of Statistics and Its Application*, *7*, 89-110.

Nerantzaki, S. D., Papalexiou, S. M., Rajulapati, C. R., & Clark, M. P. (2023). Nonstationarity in High and Low-Temperature Extremes: Insights From a Global Observational Data Set by Merging Extreme-Value Methods. *Earth's Future*, *11*(11). https://doi.org/10.1029/2023EF003506

Oldenborgh, G. J. van, van der Wiel, K., Kew, S., Philip, S., Otto, F., Vautard, R., et al. (2021). Pathways and pitfalls in extreme event attribution. *Climatic Change 2021 166:1*, *166*(1), 1–

27. https://doi.org/10.1007/S10584-021-03071-7

Papalexiou, S. M., & Montanari, A. (2019). Global and regional increase of precipitation extremes under global warming. *Water Resources Research, 55*(6), 4901-4914.

Philemon Gamet and Jonathan Jalbert. A flexible extended generalized pareto distribution for tail estimation. Environmetrics, 33(6):e2744, 2022.

Philip, S., Kew, S., van Oldenborgh, G. J., Otto, F., Vautard, R., van der Wiel, K., et al. (2020). A protocol for probabilistic extreme event attribution analyses. *Advances in Statistical Climatology, Meteorology and Oceanography*, *6*(2), 177–203. https://doi.org/10.5194/ASCMO-6-177-2020

Risser, M. D., Collins, W. D., Wehner, M. F., O'Brien, T. A., Paciorek, C. J., O'Brien, J. P., et al. (2022). A framework for detection and attribution of regional precipitation change: Application to the United States historical record. *Climate Dynamics*, *60*(3–4), 705–741. https://doi.org/10.1007/s00382-022-06321-1

Rivoire, P., Martius, O., & Naveau, P. (2021). A Comparison of Moderate and Extreme ERA-5 Daily Precipitation With Two Observational Data Sets. *Earth and Space Science*, *8*(4). https://doi.org/10.1029/2020EA001633

Seneviratne, S. I., Zhang, X., Adnan, M., Badi, W., Dereczynski, C., Di Luca, A., et al. (2021). *Weather and Climate Extreme Events in a Changing Climate. Climate Change 2021: The Physical Science Basis. Contribution of Working Group I to the Sixth Assessment Report of the Intergovernmental Panel on Climate Change*. https://doi.org/10.1017/9781009157896.013

Trenberth, K. E. (2011). Changes in precipitation with climate change. *Climate Research*, *47*(138), 123–138. https://doi.org/10.3354/cr00953

Trenberth, K. E. (2018, October 2). Climate change caused by human activities is happening and it already has major consequences. *Journal of Energy and Natural Resources Law*. Taylor and Francis Ltd. https://doi.org/10.1080/02646811.2018.1450895

Van Der Wiel, K., Kapnick, S. B., Jan Van Oldenborgh, G., Whan, K., Philip, S., Vecchi, G. A., et al. (2017). Rapid attribution of the August 2016 flood-inducing extreme precipitation in south Louisiana to climate change. *Hydrology and Earth System Sciences*, *21*(2), 897–921. https://doi.org/10.5194/hess-21-897-2017

Wang, S. Y. S., Zhao, L., Yoon, J. H., Klotzbach, P., & Gillies, R. R. (2018). Quantitative attribution of climate effects on Hurricane Harvey's extreme rainfall in Texas. *Environmental Research Letters*, *13*(5), 054014. https://doi.org/10.1088/1748-9326/AABB85

Wehner, M., & Sampson, C. (2021). Attributable human-induced changes in the magnitude of flooding in the Houston, Texas region during Hurricane Harvey. *Climatic Change*, *166*(1–2), 1–13. https://doi.org/10.1007/S10584-021-03114-Z/TABLES/2

Westra, S., Fowler, H. J., Evans, J. P., Alexander, L. V., Berg, P., Johnson, F., et al. (2014). Future changes to the intensity and frequency of short-duration extreme rainfall. *Reviews of Geophysics*, *52*(3), 522–555. https://doi.org/10.1002/2014RG000464

Xie, P., Yatagai, A., Chen, M., Hayasaka, T., Fukushima, Y., Liu, C., & Yang, S. (2007). A Gauge-Based Analysis of Daily Precipitation over East Asia. https://doi.org/10.1175/JHM583.1

Zhao, W. S.-Y., Zhao, L., Yoon, J.-H., Klotzbach, P., & Gillies, R. R. (2018). Quantitative attribution of climate effects on Hurricane Harvey's extreme rainfall in Texas. https://doi.org/10.1088/1748-9326/aabb85